# Variational Quantum Demodulation for Coherent Optical Multi-Dimensional QAM

**Toshiaki Koike-Akino, Toshiki Matsumine, Ye Wang, David S. Millar, Keisuke Kojima, Kieran Parsons**

*Mitsubishi Electric Research Laboratories (MERL), Cambridge, MA 02139, USA. koike@merl.com*

**Abstract:** We introduce a hybrid quantum-classical variational algorithms to realize quasi-ML decision of high-dimensional modulation (HDM) in fiber-optic communications, motivated by the recent advancement of quantum processors. Our Ising Hamiltonian model for demodulation is demonstrated on a real quantum processor. 

**OCIS codes:** (270.5585) Quantum processing, (060.4080) Modulation, (060.1660) Coherent communications.

## 1. Introduction

High-dimensional modulation (HDM) schemes [1–11] can improve tolerance against linear and nonlinear distortion in coherent fiber-optic communications. For instance, an improved nonlinear performance was confirmed by four-dimensional (4-D) modulation with a constant modulus property [6, 7] and 8-D modulation with a zero degree-of-polarization (DoP) property [9]. Even higher sensitivity was achieved at higher dimensions, e.g., 16-D [10] and 24-D formats [11]. However, the computational complexity for demodulation fundamentally increases with the dimension. In this paper, we introduce a new framework to demodulate HDM by leveraging a quantum processing unit (QPU) along with classical digital signal processing (DSP) as an alternative solution for an envisioned future regime of quantum supremacy [19].

Quantum computers are expected to give rise to the fourth industrial revolution because of its significant potential to accomplish efficient computations compared to traditional computers for various problems by exploiting quantum-mechanisms [19]. In the past few years, several companies including IBM, Google, and Honeywell have manufactured commercial quantum computers. For instance, IBM has released 20-qubit QPUs available to the public via a cloud service [26, 27]. It is no longer beyond imagination that noisy intermediate-scale quantum (NISQ) computers will be widely used for various real applications in the near future.

Motivated by the rapid progress of QPU development, applications of quantum-ready algorithms to wireless communication systems have been investigated in [12–16]. However, most work assume that many qubits are available without causing quantum errors, which may be beyond the capability of near-term NISQ devices. Recently, a hybrid quantum-classical algorithm having high robustness against quantum errors was proposed to solve various NP-hard problems [17,18]. The method called quantum approximate optimization algorithm (QAOA) uses the variational principle to derive probabilistic solutions by mapping onto an Ising Hamiltonian with annealing parameters. In this paper, we investigate DSP assisted with the variation quantum algorithm for demodulating HDM formats as a potential new framework to efficiently perform quasi-maximum-likelihood (ML) decision.

## 2. High-Dimensional Modulation (HDM)

We consider standard coherent fiber-optic communication systems as shown in Fig. 1, where forward error correction (FEC) codes followed by dual-polarized quadrature-amplitude modulation (DP-QAM) are used to trans-

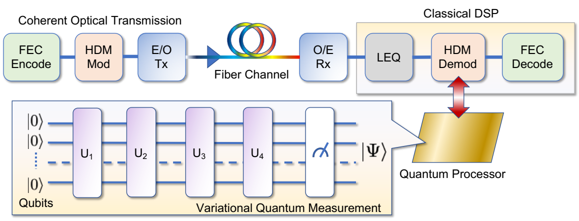


Fig. 1: QPU-assisted coherent optical transmission.

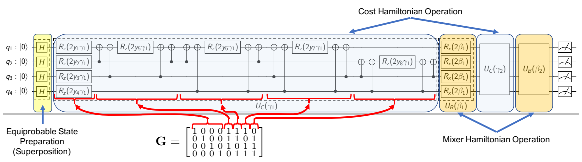


Fig. 2: Quantum gate diagram of QAOA demodulation.

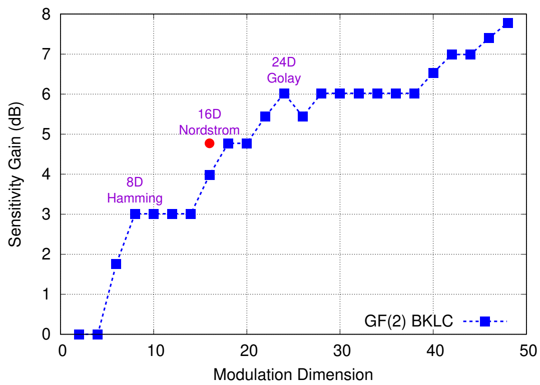


Fig. 3: Sensitivity gain of block-coded HDMs over 1-D BPSK as a function of modulation dimension.

mit digital data over optical fiber links. The channel impairments such as chromatic dispersion are compensated by DSP, e.g., carrier/phase recovery and linear equalization. In this paper, we focus on high-dimensional QAM modulation [4] to improve the noise resilience. Various HDM formats have been shown to yield benefits in the literature [1–11]. For example, 8-D modulation [9] based on extended Hamming code showed a remarkable improvement in nonlinear performance, by minimizing DoP. Fig. 3 shows an asymptotic sensitivity gain (proportional to minimum Hamming distance) of such HDMs based on best-known linear codes (BKLC) [25] for a dimension below 50. In general, the sensitivity improves as the modulation dimension increases. In fact, 24-D HDM [11] achieves an asymptotic gain greater than 6 dB, which is 3 dB better than the 8-D HDM.

One drawback of HDMs lies in the fact that soft-decision demodulation is cumbersome for higher dimensions. For approximations, one may use belief propagation or lookup tables [7] for HDM demodulation. In this paper, we introduce an alternative framework of HDM demodulation which uses QPU along with the classical DSP, shown in Fig. 1. The DSP offloads the ML calculation to the QPU, where quantum gates are applied to qubit states to approximately produce the ML decision through quantum-shot measurements. We use the recently proposed variational quantum eigensolver (VQE) [17–21] to demodulate HDMs, where quantum gates are variationally optimized by classical computers so that an average cost function is minimized to reach the solution. It was expected that VQE provides a breakthrough for NISQ devices whose quantum gates are relatively low in fidelity. Note that the hybrid quantum-classical systems in Fig. 1 are not unrealistic when considering a limited HDM dimension and the rapid advancement of QPU development in the recent years. In addition, photonic integrated circuits have a great compatibility with quantum processing as developed in integrated quantum photonics [22–24].

## 3. Variational Quantum Algorithm: QAOA

We use block-coded HDMs [4] based on BKLC [25] in Fig. 3. A hyper-cube codeword is generated by an $(n, k)$ binary BKLC, specified by a generator matrix of $\mathbf{G} \in \mathbb{F}_2^{k\times n}$, where $n$ and $k$ are the modulation dimension and information bit length, respectively. The codeword $\mathbf{c} \in \mathbb{F}_2^n$ is generated as $\mathbf{c} = \mathbf{uG}$, where arithmetic operations are based on modulo-2 and $\mathbf{u} \in \mathbb{F}_2^k$ is the binary information vector. After bipolar mapping with $\mathbf{z} = 1-2\mathbf{c} \in \{\pm 1\}^n$, the received signal over fiber links is modeled as $\mathbf{y} = \mathbf{z} + \mathbf{w}$, where $\mathbf{y} \in \mathbb{R}^n$ and $\mathbf{w} \in \mathbb{R}^n$ are the received and noise vectors, respectively. The problem of HDM demodulation is to find the codeword such that the Euclidean distance from the received signal is minimized: $\arg\min_{\mathbf{u}:\mathbf{uG}=\mathbf{c}} \|\mathbf{y} - (1-2\mathbf{c})\|^2$. The ML decision requires computations of $2^k$ codeword correlations in general. Extending recent theoretical work [21], we describe how to map the HDM demodulation problem into an Ising Hamiltonian for efficient computation by QPUs.

The proposed quantum demodulator operates on $k$-qubit space corresponding to the information bits $\mathbf{u}$, and the spin direction associates with binary $\mathbf{z}$. The objective of the quantum algorithm is to find most-likely $k$-qubit states. To do so, we consider the following cost Hamiltonian: $C = \sum_{\nu=1}^{n} y_\nu \prod_{\kappa\in\mathscr{I}_\nu^{\mathrm{c}}} \mathbf{Z}_\kappa$, where $\mathscr{I}_\nu^{\mathrm{c}}$ is a set of nonzero-element indices in the $\nu$th column of $\mathbf{G}$, i.e., $\mathscr{I}_\nu^{\mathrm{c}} = \{\kappa : [\mathbf{G}]_{\kappa,\nu} = 1\}$ where $[\cdot]_{i,j}$ denotes the element at the $i$th row and $j$th column. Since the Z-gate performs as $+|\phi\rangle$ or $-|\phi\rangle$ for $|\phi\rangle = |0\rangle$ or $|1\rangle$, respectively, maximizing the cost Hamiltonian is equivalent to the ML decision.

QAOA [17] was proposed for discrete optimization problems, such as the MaxSat and MaxCut, where the average number of satisfied clauses is maximized to find a best solution $\mathbf{z}$. Fig. 2 shows the QAOA circuit for HDM demodulation. The quantum state is first initialized by Hadamard gates to an admixing superposition state $|+\rangle^{\oplus k}$, which produces equally-likely random bits $\mathbf{z}$ once measured. For demodulation, QAOA uses two Hamiltonian operators alternately. The first cost Hamiltonian operator $U_C(\gamma)$ is defined with an angle $\gamma$ as $U_C(\gamma) = \exp(-\imath\gamma C)$. The second mixer Hamiltonian operator is defined as $U_B(\beta) = \exp(-\imath\beta B)$, where $B = \sum_{\kappa=1}^{k} \mathbf{X}_\kappa$ flips $k$-qubit independently like annealing with a parameter $\beta$. As shown in Fig. 2, the cost Hamiltonian operator is implemented with CNOT gates and Z-rotations depending on $\mathbf{G}$ while the mixer Hamiltonian operator uses X-rotations.

QAOA uses alternating quantum operator ansatz circuits of depth $p$ based on Hamiltonians $B$ and $C$ with $2p$ angle parameters $\gamma$ and $\beta$ as follows: $|\gamma,\beta\rangle = U_B(\beta_p)U_C(\gamma_p)\cdots U_B(\beta_1)U_C(\gamma_1)|\phi\rangle$. The objective of QAOA algorithm is to maximize the cost expectation $\langle\gamma,\beta|C|\gamma,\beta\rangle$ by properly choosing parameters $\gamma,\beta$. The quality of the solution improves as $p$ increases and the global optimum of cost function can be asymptotically achieved with infinite depth $p$. The calculation of the cost expectation is performed by repeated measurements with QPUs based on the variational principle. The optimization of $\gamma,\beta$ is performed by classical computers [19].

## 4. Performance Analysis

With proper factors $\beta$ and $\gamma$, the QAOA demodulation can approach ML performance. For level-1 QAOA, the optimal factors can be analytically derived according to [21]. Fig. 4 shows the landscape of cost expectation for quantum HDM demodulation. We use variational optimization over the Grove platform [28], and evaluate the optimized parameters on the Qiskit platform [26]. Fig. 5 shows the result of quantum simulations, where we can see that higher cost expectation is achieved by higher-level QAOA, whereas higher dimension does not necessarily offer higher expectation. This may be due to increased non-convexity of cost landscape, leading to higher chance to trap in local optima. This is illustrated in Fig. 6, where the optimized cost expectation for 200 independent

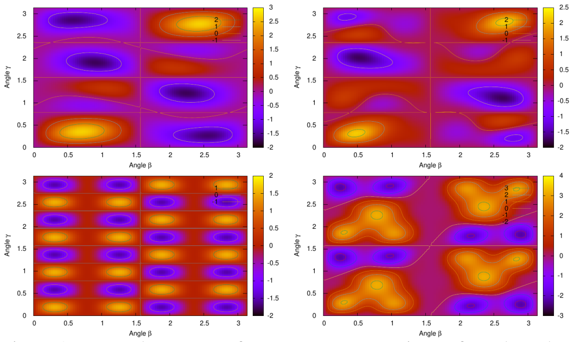

Fig. 4: Landscape of cost expectation for level-1 QAOA demodulation of 4, 6, 8, and 12-D modulations.

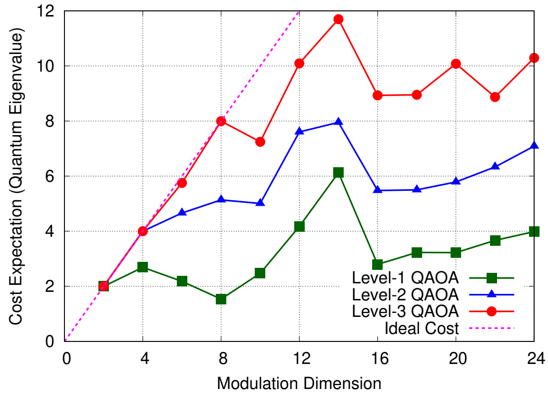

Fig. 5: Expected cost function with optimized variational angles as a function of dimension.

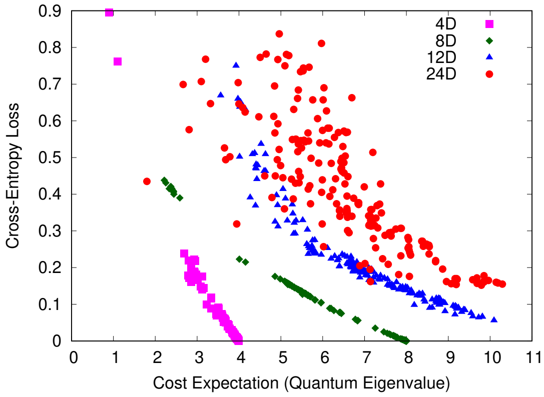

Fig. 6: Variational factor optimization for level-3 QAOA demodulation of 4, 8, 12, and 24-D HDMs.

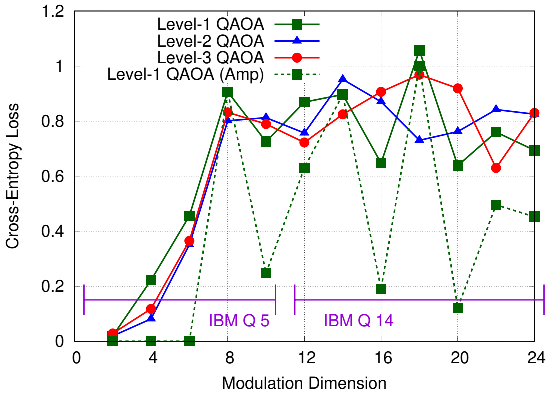

Fig. 7: Cross-entropy loss on real QPUs with variational angles optimized via ideal simulations.

optimizations is plotted. We also present the corresponding cross-entropy loss to indicate the reliability of the decision. We can see that higher dimension scatters the distributes, implying that there exist many local optima. Nonetheless, the quantum demodulation shows nearly loss-less decision, i.e., zero entropy.

The above optimization assumed ideal quantum gates, while actual QPUs experience quantum errors due to decoherence and imperfection. Fig. 7 shows the performance on real QPUs [27], IBM Q5 Tenerife and Q14 Melbourne for 2-D through 10-D HDMs and for 12-D through 24-D HDMs, respectively. The cross-entropy loss over 81,920 shots of quantum experiments is presented. Unfortunately, real QPUs exhibit considerable loss, and higher level QAOA does not improve the performance except for dimension lower than 10. Nevertheless, nearly zero loss is achieved for some cases by using wavefunction amplifications before soft-decision calculation. Here, we did not optimize variational parameters on real QPUs, and thus there remain rooms to improve on real QPUs.

## 5. Conclusion

We proposed to make use of variational quantum algorithms for HDM demodulation in coherent fiber-optic communications for the first time. Through proof-of-concept analyses, its potential in coming quantum eras was demonstrated over simulations and experiments on real QPUs. Investigating quantum-ready optical systems and algorithms will be beneficial to future advancement of ultra-high-speed fiber-optic communications.

## References


1. M. Karlsson and E. Agrell, *Optics Express* **17** 13 (2009).
2. E. Agrell and M. Karlsson, *JLT* **27** 22 (2009), pp. 5115–5126.
3. S. Betti et al., *Electronics Letters* **26** 14 (1990), pp. 992–993.
4. D. S. Millar et al., *Optics Express* **22** 7 (2014), pp. 8798—8812.
5. T. A. Eriksson et al., *JLT* **32** 12 (2014), pp. 2254–2262.
6. K. Kojima et al., *JLT* **35** 8 (2018), pp. 1383–91.
7. T. Yoshida et al., *ECOC* (2016), Th.2.P2.SC3.27.
8. M. Karlsson and E. Agrell, *JLT* **35** 4 (2017), pp. 876–84.
9. A. Shiner et al., *Optics Express* **22** 17 (2014) pp. 20366–20374.
10. T. Koike-Akino et al., *CLEO* (2015), JTh2A-59.
11. D. S. Millar et al., *OFC* (2014), M3A.5.
12. Z. Babar et al., *IEEE TVT* **64** 3 (2015), pp. 866–875.
13. P. Botsinis et al., *IEEE TCOM* **63** 10 (2015), pp. 3713–3727.
14. P. Botsinis et al., *IEEE Communications Surveys & Tutorials* (2018).
15. P. Botsinis et al., *IEEE Access* **4** (2016), pp. 7658—7681.
16. P. Botsinis et al., *IEEE Access* **4** (2016), pp. 7402–7424.
17. E. Farhi et al., *arXiv preprint* arXiv:1411.4028, (2014).
18. J. C. Patrick et al., *arXiv preprint* arXiv:1804.03719 (2018).
19. E. Farhi and A. W. Harrow, *arXiv preprint* arXiv:1602.07674 (2016).
20. S. Hadfield, *arXiv preprint* arXiv:1805.03265 (2018).
21. T. Matsumine et al., *IEEE ISIT* (2019).
22. A. Politi et al., *IEEE J. Sel. Topics Quant. Electron.* **15** 6 (2009), pp. 1673–1684.
23. J. L. O'Brien et al., *Nature Photonics* **3** 12 (2009), pp. 687–695.
24. A. Peruzzo et al., *Nature Communications* **23** 5 (2014), p. 4213.
25. W. Bosma et al., *J. Symbolic Comput.* **24** (1997), pp. 235–265.
26. G. Aleksandrowicz et al. (2019), DOI:10.5281/zenodo.2562110.
27. 'IBM Q,' https://www.research.ibm.com/ibm-q/, accessed April 2019.
28. R. Smith et al., *arXiv preprint* arXiv:1608.03355 [quant-ph] (2015), https://arxiv.org/abs/1608.03355.